A Novel Way of Enhancing the Electrical and Thermal Stability of Conductive Epoxy Resin–Carbon Black Composites via the Joule Heating Effect for Heating-Element Applications

Farid El-Tantawy,[1,2] K. Kamada,[3] H. Ohnabe[2]

[1]*Department of Physics, Faculty of Science, Suez Canal University, Ismailia, Egypt*
[2]*Department of Biocybernetics, Faculty of Engineering, Niigata University, 8050, Ikarashi 2-nocho, Niigata 950-2181, Japan*
[3]*Graduate Schools of Science and Technology, Niigata University, 8050, Ikarashi 2-nocho, Niigata 950-2181, Japan*

Received 6 June 2001; accepted 19 November 2001

ABSTRACT: The influence of Joule heating treatments and carbon black (CB) on the electrical and thermal behavior of epoxy resin composites is well described in this article. The effect of CB and Joule heating on network structure characteristics, such as shrinkability, interparticle distance between conductive particles, crosslinking density, hardness, thermoelectric power, thermal conductivity, the thermal expansion coefficient, and scanning electron microscopy, of epoxy composites was investigated. The electrical conductivity (σ) of epoxy resin correlated with the volume fraction of CB and Joule heating treatment. σ increased continuously with increasing CB content, and Joule heating increased the level of σ, which makes it attractive for electronic utilization. The σ for fresh and Joule heating samples was recorded during heating–cooling cycles. The conduction mechanism of σ for epoxy composites was identified. The activation energy and hopping energy for two batches of epoxy as a function of CB content were estimated. The hopping distance, the state density at the Fermi level, and the radius of localized wave function versus CB content were evaluated. The current–voltage–temperature characteristics of fresh and Joule heating samples of epoxy composites were demonstrated. The thermal reliability was tested by means of temperature–time characteristics when certain applied power was on and off for several cycles. The specific heat and amount of heat transfer by radiation and convection were calculated based on the energy balance model for two batches. The results indicate that the Joule heating effect is a very effective and prospective way of enhancing the electrical and thermal stability of epoxy–CB composites for consumer use as heaters and in other electronic areas such as electromagnetic shielding effectiveness.
 J Appl Polym Sci 87: 97–109, 2003

Key words: composites; resins; interfaces; activation energy

INTRODUCTION

Commercially used epoxy resins find their applications in a variety of fields, such as in the electrical and electronics areas and for adhesives, oil wells, protective coatings, and composites, due to their outstanding physicochemical properties, including electrical, mechanical, thermal, and chemical resistances.[1] Electrically conducting polymer composites have attracted a great deal of scientific and commercial interest during the last few years.[2] The development of conductive polymers with good physical stability are desirable for the electronic industry.[3] Fillers such as carbon black (CB), graphite, or others are widely used in polymer composites to provide characteristics to suit a particular application.[4] Filled polymer composites have wide applications, such as for flooring materials to dissipate static electricity charges,[5] electromagnetic shielding,[4] self-regulating heaters,[6] and electrical circuit protection.[7] It is well known that the electrical and thermal properties of conductive polymer composites are strongly influenced by factors such as type, size, content, and shape of the filler and preparation techniques.[8] However, one of the key problems related to the potential application of conductive polymers is stability and reproducibility (i.e., reliability). The most promising approaches to the solution of this problem are a long annealing time,[9] the reprocessing of green polymer,[10] the addition of inhibitor additives,[10] the modification of the molecular structure,[11] irradiation, and others.[1–3] From a technological point of view, all of these methods are inconvenient, expensive, and time consuming. Whenever such polymer composites are used as thermistors for electrical heaters, they are subjected to repeated thermal cycles, and it becomes necessary to understand how electrical conductivity

Correspondence to: F. El-Tantawy, Department of Physics, Faculty of Science, Suez Canal University, Ismailia, Egypt (faridtantawy@yahoo.com).

Journal of Applied Polymer Science, Vol. 87, 97–109 (2003)

(σ) changes with repeated thermal cycles and applied power; especially in electrical technology, a higher stability is required under severe operating conditions. So, future applications of these materials strongly depend on the success of improving their stability with respect to thermal cycles.

To our knowledge, the effect of Joule heating treatment on the electrical and thermal stability of epoxy–CB composites has not yet been reported. With this taken into consideration, the objective of this research was to present new data on the effect of Joule heating on the electrical and thermal stability of epoxy–CB composites. The effect of CB content on the network structure of epoxy composites was investigated. To elucidate the effect of Joule heating on the electrical and thermal stability of epoxy–CB composites, σ was studied as a function of temperature cycles. Also, thermal stability was examined by means of temperature–time dependence with an applied fixed electric field on and off for several cycles. The results were very promising, and it was possible to obtain high temperature sensitivity at low power and a good stability of characteristics. In conclusion, the Joule heating effect is an effective and prospective way for improving the thermal and electrical stability of these composites.

EXPERIMENTAL

An epoxy resin with the commercial name Epcoat 835 and hardener type B002W (mixing ratio = 100:25 wt %), both from Yuka Shell Epoxy Chemical Co., Tokyo, Japan) were used as a matrix system for the composites. The furnace CB with a particle size of 2 μm and a surface area of 12 m^2/g was used as a conductive filler component in the composite. All of the chemicals were used as received. The CB–epoxy weight ratios for the five batches were 4/6, 5/5, 6/4, 6.5/3.5, and 7/3, abbreviated as F4/6, F5/5, F6/4, F6.5/3.5, and F7/3, respectively. The green epoxy/hardener with a different content of CB was prepared with a centrifuging mixer (Matsuo, Japan); for 1 min at room temperature. The bulk samples of the composite were obtained by casting of the green composites on a Teflon mold. Mosaic gold–copper electrodes were embedded into samples during the preparation process to reduce the sample electrode contact resistance.12 Then, the epoxy–CB composites were cured in an electrical oven at 90°C for 13 h. A morphology study of the epoxy composites was conducted with scanning electron microscopy (SEM; JSM-5310 LVB, Jeol, Tokyo, Japan). Hardness (Hv) was determined with a universal testing machine (ASTM D 2240 78; Osaka, Japan). The density of the epoxy–CB composites was measured with the floating method.1 The thermal expansion coefficient (TEC) was measured by the dilatometer technique. For the Joule heating effect, a power of about 1 W for 3 h was applied to the cured epoxy–CB composite samples. The thermoelectric power (TEP) was measured through the gold–copper leads by a Yokogawa portable data logger type P030 (Tokyo, Japan). For the measurement of the power-dependent temperature, samples were placed in a controlled chamber at 20°C. A computer-controlled the temperature for each applied power. For the measurement of thermal conductivity (λ), electrical power was applied to the sample, and once the thermal equilibrium was reached, the temperature was read by a thermocouple. The electrical power was then changed to obtain a set of data. λ was obtained as a derivative of W/cm K. σ was measured through the specimen thickness. The specimen with the attached copper electrodes was placed in a special chamber where the temperature was controlled in accordance with a desirable basic program. The heating rate during electrical measurements was 3°C/min. Original software was used to measure σ with temperature. The software maintained the recording of σ with a temperature interval of 2°C. σ was evaluated from the measured resistance divided by a geometrical factor t/A, where t and A are the thickness and area of the testing samples, respectively. The circuit used for measuring current–voltage characteristics was described elsewhere.13 The structure of the samples was obtained at room temperature with X-ray diffraction (XRD) obtained with a Rigaku-DXG1 diffractometer (λ = 0.70930 Å) (Osaka, Japan).

RESULTS AND DISCUSSION

Network structure

To solve some problems related to the material engineering itself and nondestructive quality control, we found it necessary to make an analytical description of the network structure as a function of the filling phase because the physical properties critically depended on the phase continuity, interfacial area, and crosslinking density (CLD). Therefore, it was worth studying the influence of CB content and the Joule heating effect on network structure and phase morphology. This would help us better understand the microstructure core of epoxy–CB composites.

The shrinkability (S) of epoxy–CB composites was calculated according to the equation:[14]

$$S = \frac{\rho_g^{-1} - \rho_t^{-1}}{\rho_g^{-1}} \times 100 \quad (1)$$

where ρ_t is the density on curing for a time t, and ρ_g is the green density of the epoxy.

The interparticle distance (ω) between conductive particles was calculated by the equation:[9]

$$\varpi = -D\left[\left(\frac{k\pi}{6V_r}\right)^{1/3} - 1\right] \quad (2)$$

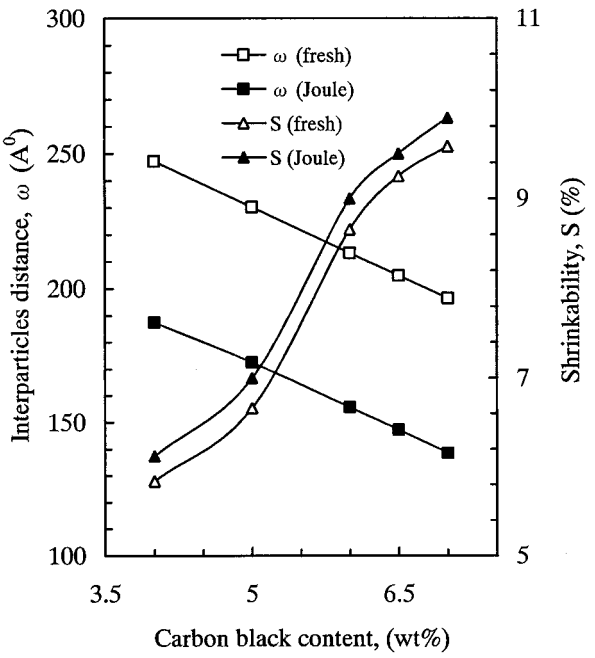

Figure 1 ω between CB particles and S versus CB content for fresh and Joule heating samples for epoxy–CB composites.

where D is the CB particle diameter, $k = 1$ for cubic packing, and V_r is the volume fraction of the epoxy network and is given by the following equation:[1]

$$V_r = V_{r0}(0.56e^{-\phi} + 0.44) \quad (3)$$

where V_{r0} is the volume fraction of epoxy in the swollen samples and ϕ is the volume fraction of CB content in the cured composites.

The relationship between S and ω as a function of CB content for fresh and Joule heating samples is displayed in Figure 1. The S curves were characterized by a typical sigmoid-shaped profile and increased with increasing CB content. This could be explained by the fact that the CB particles filled the free volume and increased the packing density of the epoxy matrix. The level of the Joule heating sample for S was higher compared to the that of the fresh sample. This was ascribed to the fact that Joule heating increased the interfacial activity of CB particles in the epoxy matrix. However, ω decreased with increasing CB content for two samples, and the level of the Joule heating sample was lower compared to that of the fresh one. We believe that the Joule heating allowed execution of interchain hopping, which led to an increasingly effective dimensionality and decreased the interchain width within the epoxy matrix.

CLD of epoxy–CB composites was determined by the following equation:[4,15]

$$\mathrm{CLD} = -\frac{M_e[-\ln(1 - V_r) - V_r - \chi V_r^2]}{2.3\left(\frac{0.5\rho_g RT}{\mathrm{CLD}} + 0.78 \times 10^6\right)2V_k V_r^{1/3}} + 1 \quad (4)$$

where R is the universal gas constant, T is the absolute temperature, M_e is the average molecular weight of the epoxy before curing, V_k is the volume fraction of the solvent, and χ is the Flory–Huggins interaction parameter between the solvent and epoxy and is about 0.38.[15]

The variations of CLD and H_v versus CB content for two batches (i.e., fresh and Joule heating samples) of the epoxy–CB composites are plotted in Figure 2(a). CLD increased with increasing CB content; this indicates that CB increased the interchain connectivity among conductive phases. For the Joule heating batch, CLD was higher than for the fresh one. We propose that Joule heating improved the ordering of interchain connectivity and created a repulsive force between CB particles, which contributed to interpenetrating and homogeneous dispersion of CB particles into the epoxy matrix. This led to an increase in the CLD within the epoxy matrix with Joule heating. For confirmation on this thinking, the XRD analysis for pure epoxy and fresh and Joule heating samples F6/4 is shown in Figure 2(b). In comparison between the fresh and Joule heating samples, it is clear that the intensity of the Joule heating sample was higher than that of the fresh sample. This strongly indicates that the Joule heating treatments enhanced the texturing and ordering of the microstructure core of the epoxy matrix. To clarify the repulsive force between CB particles due to Joule heating, let us consider the electrical operation circuit of conductive particles inside epoxy matrix that is described by the electric equivalent circuit in Figure 2(c). We speculated that at a high electric field (i.e., Joule heating), the whole polymer matrix was heated by Joule heating, and therefore, the polymer matrix contained a link and separate conductive particles. At a high electric field, the separated conducive particles may have had electrostatic capacity; therefore, the conductive particles may have charged, as in the circuit in the Figure 2(c). The positive charged conductive particle may have generated Coulomb attractive forces among the separated particles and repulsive forces among the linking particles, and thus, resistance may have decreased and/or increased. This can be explained by the fact that the charge carriers in the sample moved easily to the positive electrode, and therefore, the resistance in that side decreased. However, the carriers vacancy concentration increased at the negative potential pole, resulting in an increasing resistance. Thereby, we concluded that the increase of conductivity was clearly generated by a repulsive force at a high applied potential (i.e., Joule heating treatment) in the epoxy matrix. However, the increase of H_v with CB content and Joule heating implies that

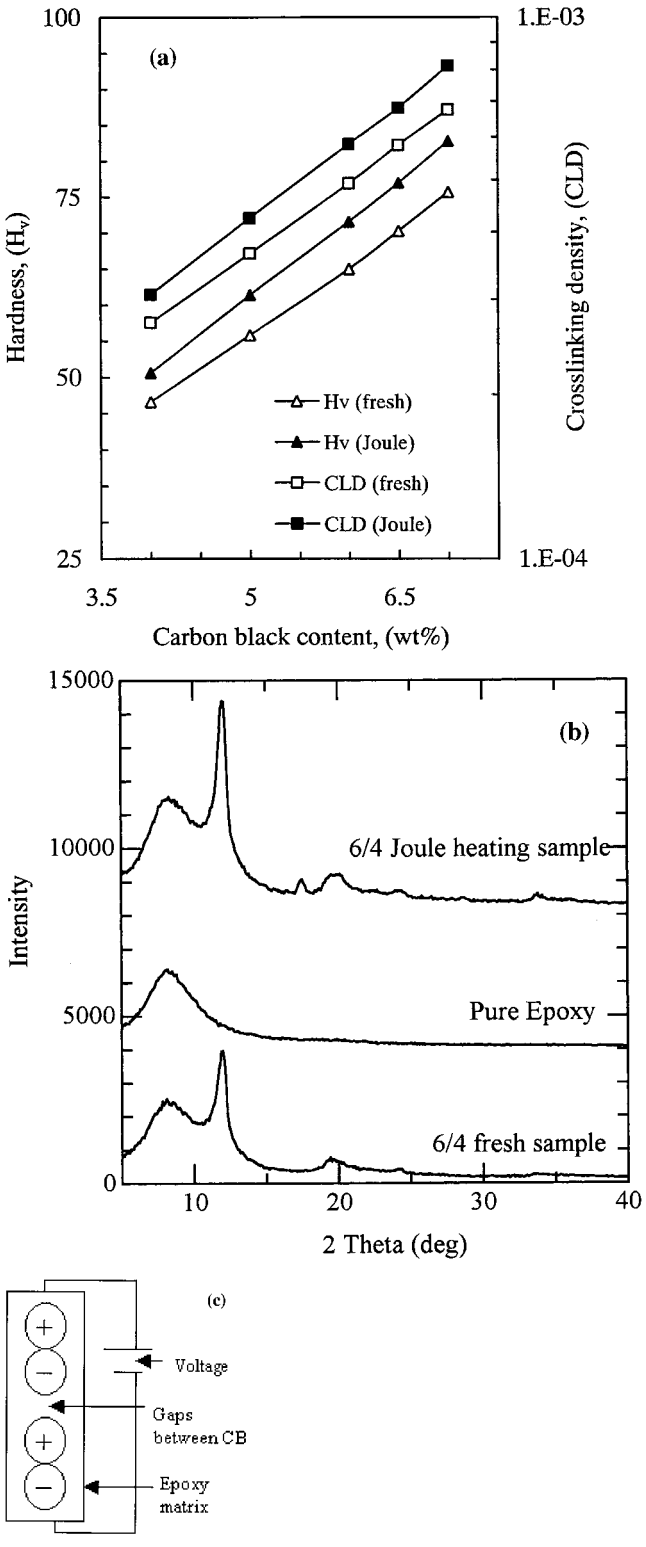

Figure 2 (a) Variation in H_v and CLD against CB content for two batches of epoxy–CB composites, (b) XRD analysis of pure epoxy and sample F6/4 for fresh and Joule heating, and (c) electrical equivalent circuit of CB within the epoxy matrix.

the CB and Joule heating reduced the creep of CB particles and minimized the strain energy within the epoxy matrix.[5,8] To confirm our thinking on the previous discussion, λ, TEP, and TEC for epoxy–CB composites of two batches are depicted in Figure 3. As shown, λ and TEP increased with increasing CB content, and the level of the Joule heating batch was higher than that of the fresh batch. Although TEC decreased with increasing CB content, the level of the Joule heating batch was lower than that of the fresh batch. This could be explained by the fact that the Joule heating and CB increased the thermal resistance and network structure density of the epoxy matrix.

Morphology study

To compare the SEM photographs of fresh and Joule heating samples, we analyzed samples F6/4 and F7/3. Figure 4(a,b) shows the SEM of fresh samples F4/6 and F7/3, respectively. In general, the nonspherical and irregular shape of the CB grains with sizes ranging from 2 to 8 μm was evident, and the CB particles depicted a fairly uniform distribution in the epoxy matrix. As shown in Figure 4(a), the CB particles were nonuniform and had poor dispersion and weak wettability into the epoxy matrix. In addition, the CB particles were isolated, and the microstructure was still dominated by the epoxy matrix; CB particles were in closer proximity. However, in Figure 4(b), that is, sample F7/3, the CB particles showed good connectivity and dispersion into the epoxy matrix. Also, the CB particles began to agglomerate in the epoxy matrix, and interchain link formation became significant. Figure 4(c,d) shows the SEM of Joule heating samples F4/6 and F7/3, respectively. It is shown that Joule

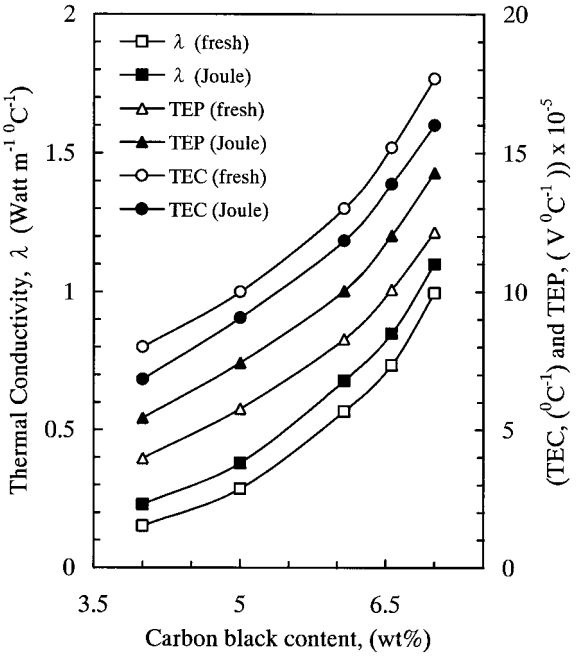

Figure 3 Variation in λ, TEP, and TEC against CB content for two batches of epoxy–CB composites.

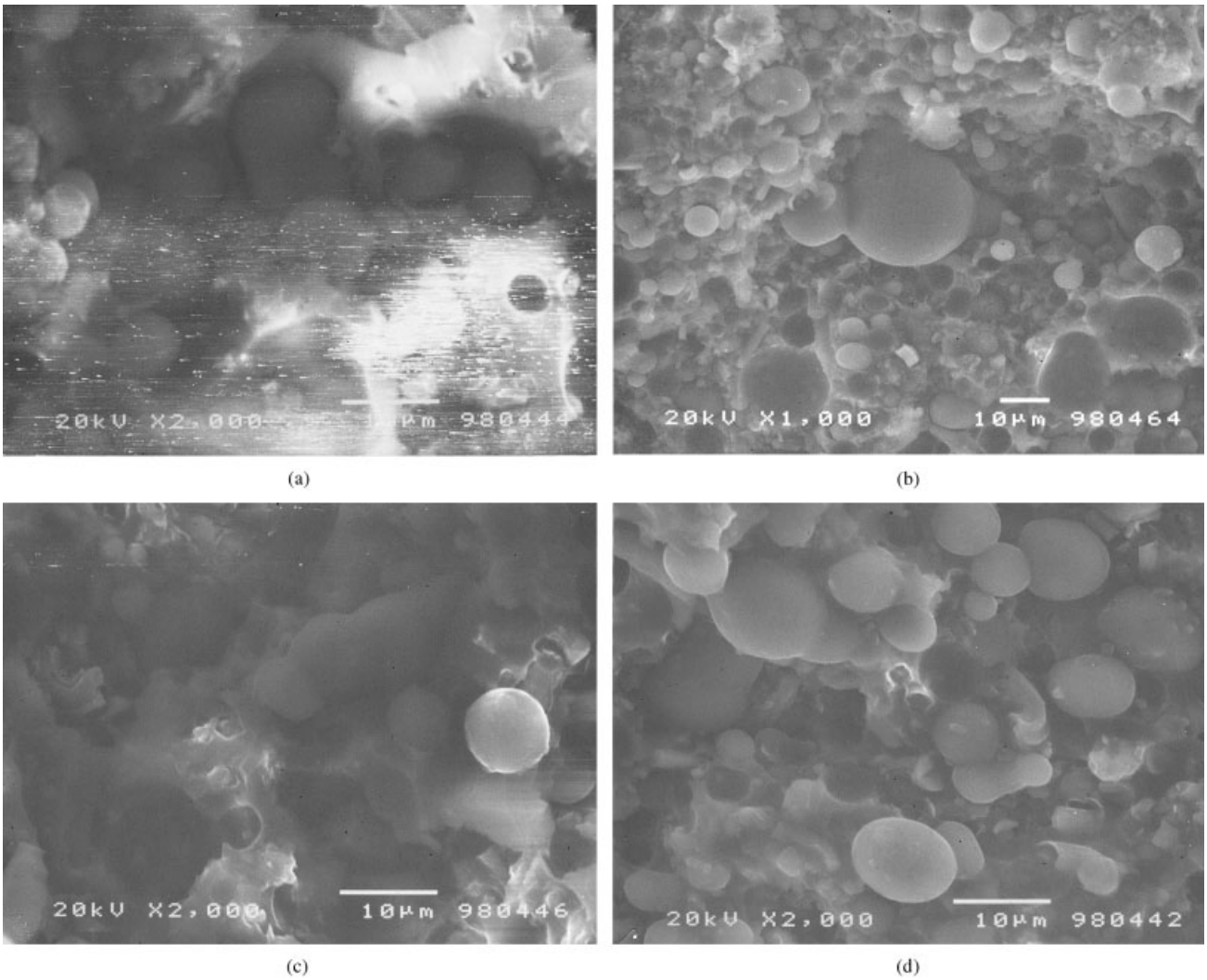

Figure 4 SEM pictures of epoxy–CB composites: (a) fresh sample F4/6, (b) fresh sample F7/3, (c) Joule heating sample F4/6, and (d) Joule heating sample F7/3.

heating increased the interfacial adhesion, ordering, and dispersion of CB particles in the epoxy matrix.

With these considerations of microstructure, we could predict that the network structure density would increase, whereas σ would increase with increasing CB content and Joule heating treatment. Therefore, Joule heating had a positive effect on the physicochemical properties of the epoxy composites, as confirmed previously.

Conductivity characteristics

Percolation threshold

The direct current (DC) σ of epoxy–CB composites was related to the formation of a network of CB particles within the epoxy matrix. The formation and nature of this network depended entirely on the size of CB; its separation, dispersion, and interface; and the volume fraction of CB particles in the matrix. The effect of CB content on the σ at room temperature about 25°C is shown in Figure 5. It is clear that σ increased continuously with increasing CB content for the epoxy matrix. When the volume fraction of CB particles was less than 4 wt %, the conducting CB particles formed isolated islands within the insulating epoxy matrix, there was no physical contact between CB particles, and of course, σ was activated.[4] With increasing volume fractions of CB particles (more than 4 wt %), the conductive islands became larger, and the widening between CB particles became closer, which culminated in a reduction in the activation energy (E_a) between conductive sites. Therefore, the density of the network paths was increased in these composites. As a consequence, σ showed a continuous increase.

However, the critical percolation threshold of these composites was about 0.40. The level of σ of the Joule heating batch was higher than that of the fresh batch, as shown in Figure 5. This implies that Joule heating

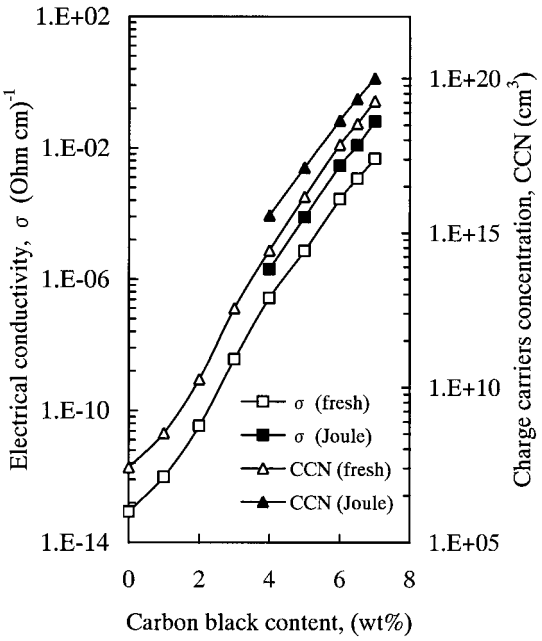

Figure 5 Relationship of σ and charge carriers' concentration with CB percentage for fresh and Joule heating samples of epoxy–CB composites.

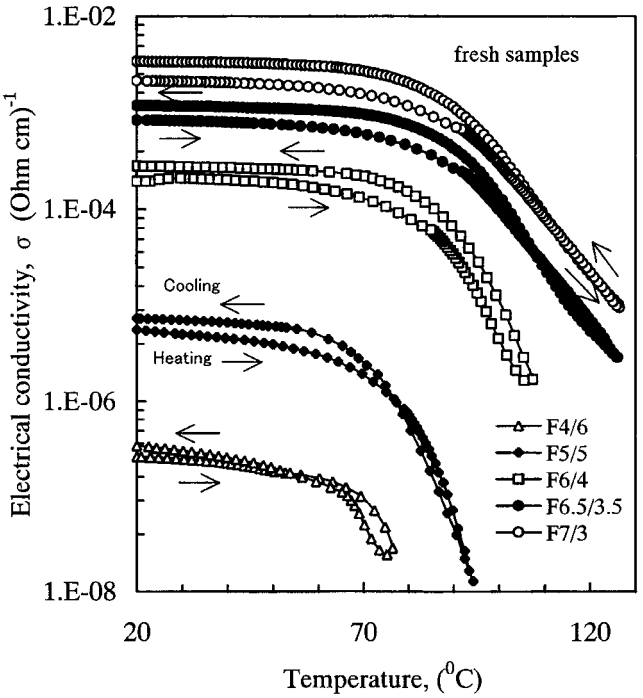

Figure 6 Effect of heating–cooling cycles on the volume conductivity for fresh samples of epoxy–CB composites.

increased and aligned the conductive network channels within the epoxy matrix. Also, we thought the increase in σ of the Joule heating batch may have been due to the Coulomb repulsive force between CB particles and an increase in the polarization density into the epoxy matrix.

Confirmation of the charge carrier's concentration (CCN) into epoxy matrix could be obtained with the equation:[14]

$$CCN = \frac{\sigma}{\mu e} \tag{5}$$

where μ is the electron mobility (about 0.6 cm^2/V s) and e is the electron charge.

The increase of CCN with increasing CB content and Joule heating as shown in Figure 5 reflects the fact that CB acted as a charge reservoir and Joule heating enhanced the architectural structure of the conductive filaments and/or acted as a pinning center effect (i.e., increasing the dipole moment density) within the epoxy matrix.[1]

However, the percolation curve in Figure 5 could be empirically described by the polynomial equation in the form:

$$\sigma = -2 \times 10^{-3}\phi^2 + 9 \times 10^{-4}\phi - 4 \times 10^{-4} \tag{6}$$

In conclusion, the previous equation allowed us to predict the variation of conductivity with CB content and was useful for the members of a planning group for this composite.

Conductivity–temperature dependence

The σ versus temperature ($\sigma - T$) curves for fresh and Joule heating batches are plotted and compared in

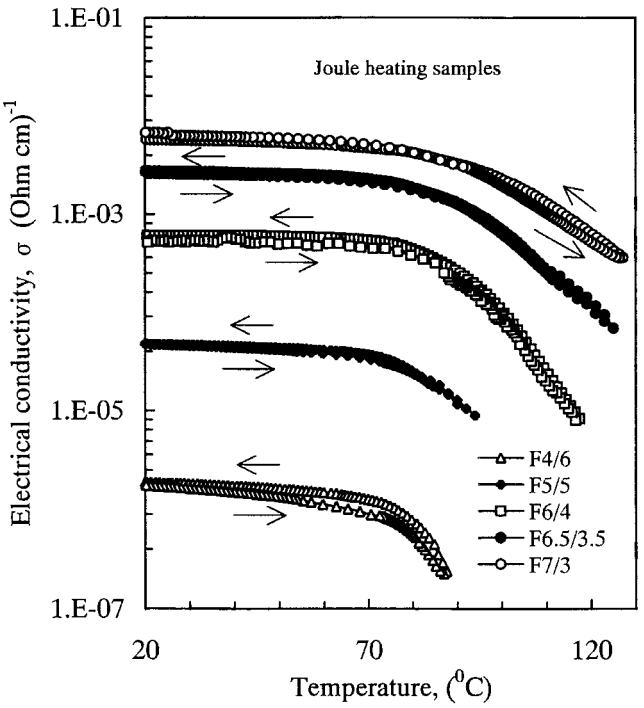

Figure 7 Effect of heating–cooling cycles on the volume conductivity for Joule heating samples of epoxy–CB composites.

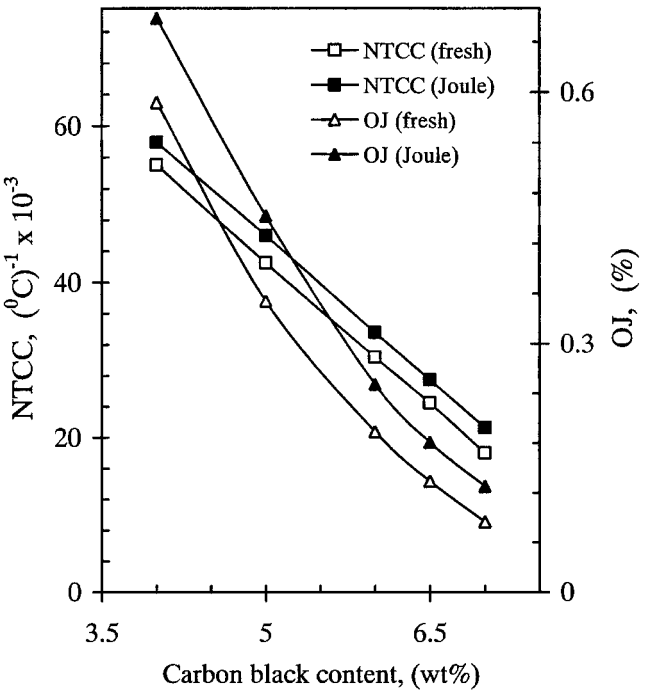

Figure 8 Variations in OJ and NTCC versus CB content of epoxy composites for two batches.

Figures 6 and 7, respectively, for the epoxy–CB composites. It is clear that the value of σ increased with increasing of both CB and Joule heating. The increase in σ level with increasing CB content may have resulted from the change of microstructure, that is, the exaggeration of conductive domains into epoxy matrix. In addition, the level of σ of the Joule heating batch was higher than that of the fresh batch. This was ascribed to the Joule-heating-induced conformational change of the molecular structure and to an increase in the dipole moment within the epoxy matrix.[1]

Generally, σ decreased (i.e., resistivity increased) with increasing temperature for the two batches. The probable reason for this phenomenon could be explained in the following way. With increasing temperature, the epoxy matrix expanded, and the gap width between CB particles increased. Moreover, the viscosity of epoxy matrix was very low at high temperatures, leading to decreased diffusion of the charge carrier mobility within the epoxy matrix. Therefore, the increase in gap width and the decrease of the charge carrier's mobility with temperature caused a marginal decrease in σ.

The $\sigma - T$ curves of the epoxy samples served to help us determine the behavior of the samples as a heating element by evaluation of the two parameters, namely, order of negative temperature coefficient jump percentage (OJ), given by the following equation:[12]

$$OJ(\%) = \log(\rho_{max} - \rho_{min}) \times 100 \quad (7)$$

where ρ_{max} and ρ_{min} are the maximum and minimum resistivity, respectively, and

$$NTCC = \pm\left(\frac{d\sigma}{\sigma_0}\right)\left(\frac{1}{dT}\right) \quad (8)$$

where NTCC is the negative temperature coefficient of conductivity and σ_0 is the initial conductivity.

The variations of OJ and NTCC versus CB content in epoxy composites for the two batches are depicted in Figure 8. It is clear that the OJ and NTCC for the two batches decreased with increasing CB content and were improved by the Joule heating effect. This association to Joule heating increased the CCN and reduced the potential barriers among the conductive phases. Also, the decreases in OJ and NTCC with Joule heating treatment indicate that the Joule heating refined the orientation and connectivity of the molecular chains within the epoxy matrix.

Hysteresis effect

To check for the stability of the electrical characteristics of the fresh and Joule heating samples, we performed conductivity measurements with nine cycles. A comparison of the conductivity versus temperature for the nine cycles for fresh and Joule heating samples F7/3 is plotted in Figure 9. For the fresh sample, a dramatic increase in σ was observed by two orders of magnitude after each cycle. This could be explained by

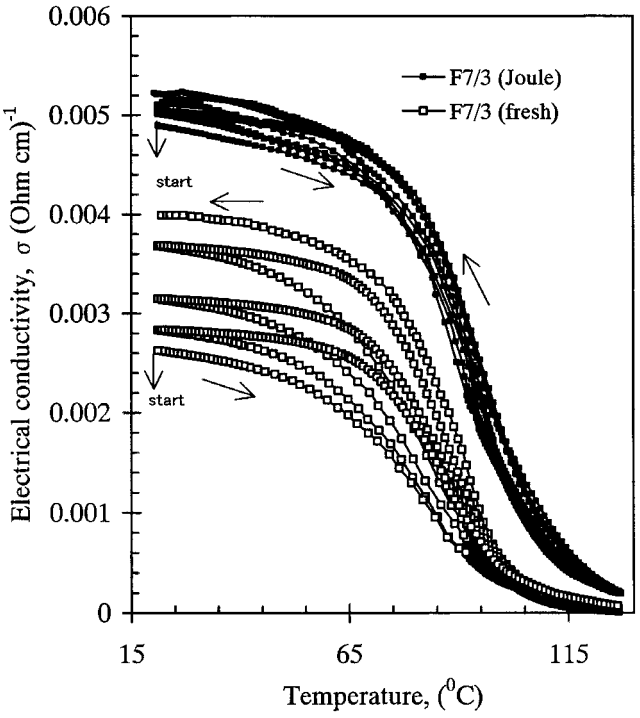

Figure 9 Conductivity versus temperature for nine cycles for fresh and Joule heating samples F7/3.

the fact that the mobility of charge carriers increased with time, too, due to the enhancement of the microstructure core of the epoxy matrix, which resulted in an increase in conductivity. Also, thermal aging may have reduced the particle size of CB grains and improved the thermodynamic stability in the epoxy matrix. The level of the hysteresis loop for the fresh sample was higher than that of the Joule heating sample during the cooling process. This could be explained by the fact that during the cooling process, some nonuniform defect concentration was established because of the time-dependent diffusion phenomena.[4] Because the diffusion coefficient decreased with temperature, the defect concentration became frozen with an inhomogeneous distribution at room temperature.[1] For this reason, the behavior of conductivity showed an irreversible process for the fresh batch. On the contrary, the Joule heating batch showed a very slight hysteresis loop after each cycle. The main reason for this was that the heat energy generation (i.e., the increase in the bulk sample temperature) by Joule heating assisted the mobilization of charge carriers, brought the chain vibration, and filled the defects concentration within the epoxy matrix.[4]

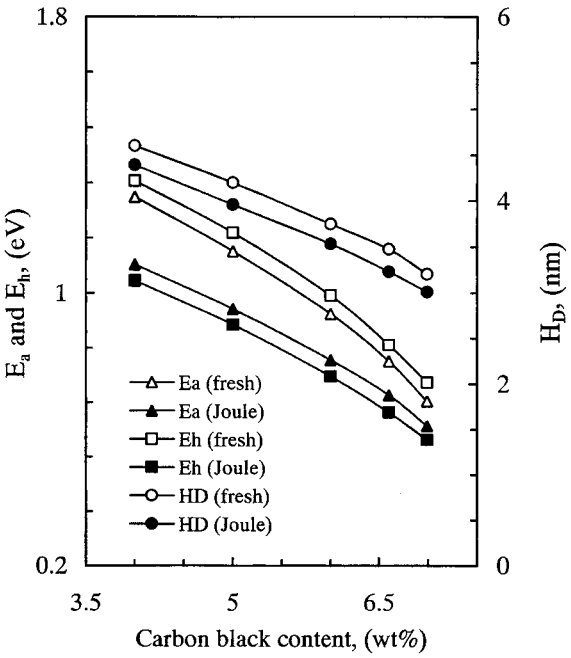

Figure 10 Variation in E_a, E_h, and H_D against CB content for fresh and Joule heating samples of epoxy–CB composites.

Conduction mechanism

To obtain better insight into the electrical transport in the epoxy–CB composites, we found it rewarding to evaluate E_a over a large range of $\sigma - T$ dependence. The variation of σ with temperature is expressed by the equation:[6]

$$\sigma = \sigma_p \exp - \left(\frac{E_a}{K_B T}\right) \tag{9}$$

where ρ_p is the preexponential factor that depends on the type of CB and K_B is the Boltzmann constant.

E_a of the conduction process was calculated from the slope of the straight line part of σ against $(1/T)$, which was equal to $(-E_a/K_B)$, and the obtained values of E_a versus CB content for two batches is plotted in Figure 10. The hopping energy (E_h) could be calculated according to the following formula:[6]

$$\sigma\sqrt{T} = A \exp - \left(\frac{E_h}{K_B T}\right) \tag{10}$$

where A is a constant.

The estimated value of E_h as a function of CB content for two batches is displayed in Figure 10. It is clear from Figure 10 that the E_a and E_h decreased with increasing CB content, and the levels of E_a and E_h for the Joule heating batch were lower than for the fresh batch. This may have been because the Joule heating reduced the potential barriers among the conductive phases within the epoxy matrix. The value of E_h was quite close to the value of E_a. This means that the conduction mechanism in the epoxy–CB composites was governed by a small polaron hopping conduction mechanism.[1,10]

The $\sigma - T$ can be described by the Mott equation:[15]

$$\sigma(T) = \sigma_0 \exp\lfloor -(T_0/T)^{1/4} \rfloor \tag{11}$$

where the constants T_0 and σ_0 are given by

$$T_0 = \frac{\lambda \alpha^3}{K_B N(E_F)} \tag{12}$$

$$\sigma_0(T) = e^2 H_D^2(T) \nu_0 N(E_F) \tag{13}$$

where

$$H_D = \left(\frac{9}{8\pi\alpha K_B T N(E_F)}\right)^{1/4} \tag{14}$$

where H_D is the hopping distance, e is the electronic charge, $N(E)$ is the state density at the Fermi level, α is the inverse rate of fall-off of the wave function (α−1 is the radius of localized wave function), λ is a dimensionless constant with a value of −18.1, and ν_0 is the jump rate prefactor with a value of 10^{13} S^{-1}.

For the evaluation of $N(E)$ and H_D, we used the following equations:[15]

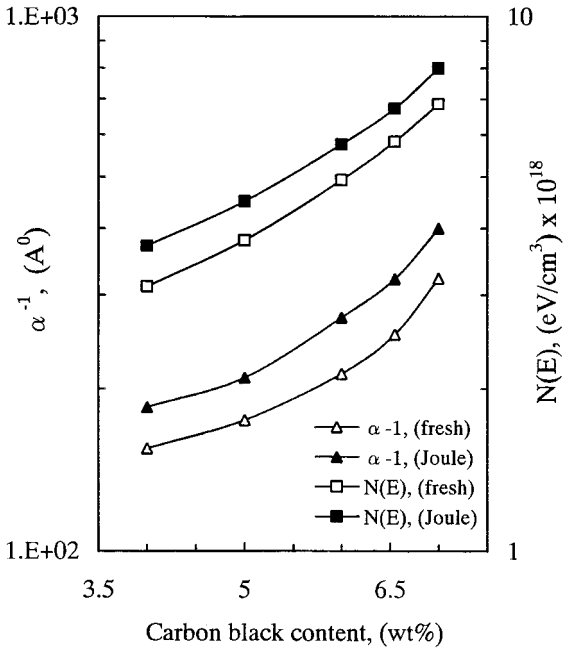

Figure 11 Variations in $N(E)$ and α^{-1} versus CB content for two batches of epoxy composites.

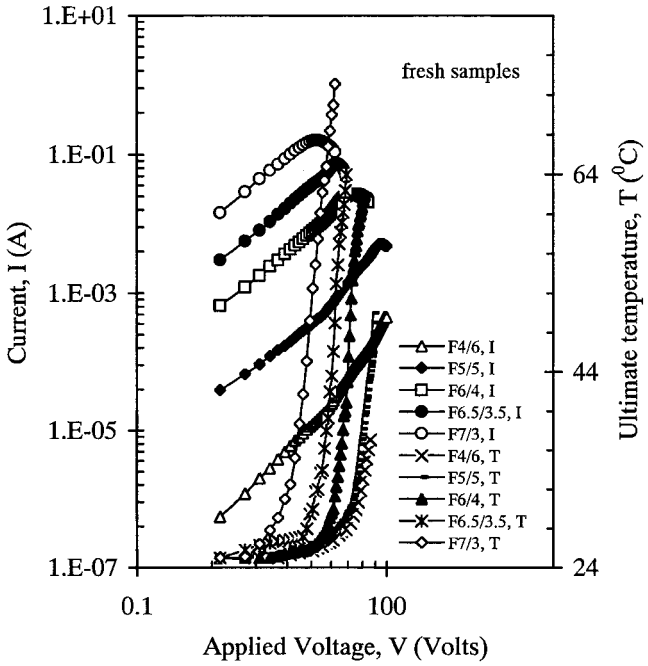

Figure 12 Current–voltage–temperature characteristics of epoxies with different contents of CB for fresh samples of epoxy composites.

$$N(E_F) = (1.966 \times 10^{48}/\upsilon_0^3) \times [(\sigma_0\sqrt{T})^3\ \sqrt{T_0}] \quad (15)$$

$$\alpha^{-1} = (21.22 \times 10^{13}/\upsilon_0)[(\sigma_0\sqrt{T})^3\sqrt{T_0}]^{-1} \quad (16)$$

The estimated values of H_D versus CB content for two batches are depicted in Figure 10. The variations of $N(E)$ and α^{-1} versus CB content for two batches are plotted in Figure 11. It is clear that H_D, $N(E)$, and α^{-1} increased with increasing CB content and Joule heating. This was attributed to the fact that the bipolaron state was bound to charged defects such as the end groups of main chains of the epoxy matrix.[15] From the previous results, we judged that the charge carrier transport in the epoxy matrix occurred via the small polaron hopping process among broadened bipolaron states in the epoxy chains.[9]

Current–voltage–temperature characteristics

Figures 12 and 13 present the current–voltage–temperature characteristics of epoxies with different contents of CB for fresh and Joule heating samples, respectively. At low applied voltage, current-voltage (I–V) exhibited linear resistance, indicating Ohmic (i.e. linear) behavior without any remarkable change in the sample temperature. In fact, the samples behaved as an Ohmic resistor in which the current density was controlled by a thermal generation electric field across the gap between the conductive particle electrons and/or holes. However, with increasing electric field, the behavior of I–V changed from linear to non-Ohmic (i.e., nonlinear). This may have been due to the change in the percolation path across the epoxy matrix. Increasing the electric field above a certain voltage, namely, the hot voltage (V_h), depended on CB content, leading to an increase in the Joule heating effect and, consequently, an increase in the sample temperature

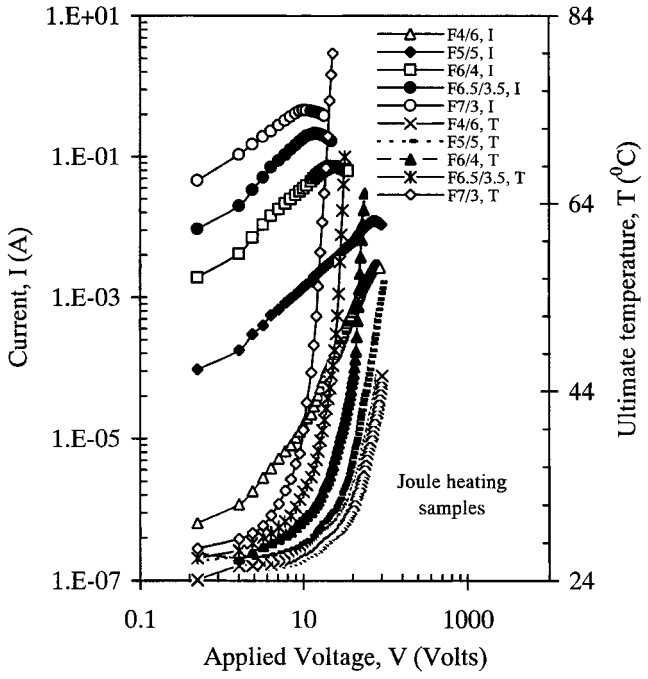

Figure 13 Current–voltage–temperature characteristics of epoxies with different contents of CB for Joule heating samples of epoxy composites.

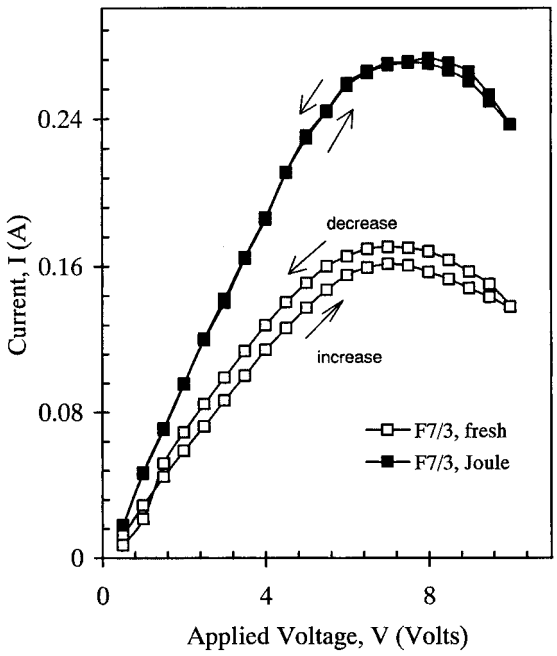

Figure 14 Current–voltage characteristics of fresh and Joule heating samples F7/3 during applied voltage forward and reverse cycles.

and a decrease in the current, that is, a negative resistance [$(dI/dV) < 0$]. We speculated that the negative resistance was generated by a Coulomb attractive force at a high applied field in the epoxy composites and that the negative resistance (i.e., resistance increased) was mainly due to a relaxation in pressure at the neck surface of the conductive particles and a break in filaments interlinked by conductive particles at a high electric field.[1,13]

The magnitude of current for the Joule heating batch was higher than that of the fresh batch, and V_h shifted to a lower voltage. This indicates that the Joule heating matured the microstructure core of the epoxy matrix.

As a test of the stability, the *I–V* curve for one cycle under an applied field for two batches of sample F7/3 are depicted in Figure 14. It is clear that the fresh batch had a higher hysteresis loop compared to the Joule heating batch. This argument supports the notion that Joule heating enhanced the thermal stability of the epoxy matrix.

In general, the *I–V* curves of the epoxy–CB composites exhibited nonlinear voltage limiting (V_l) behavior (i.e., deviation from Ohmic to non-Ohmic). The non-Ohmicity coefficient (ψ) is defined by the relation:[15]

$$I = \frac{NV^{\psi} + \delta(V - V_l)}{(V - V_l)} \tag{17}$$

where N is the proportionality constant and δ is the uniformity factor ($\alpha = 0$ for perfectly uniform samples and $\alpha > 0$ for nonuniform samples).

The calculated values of ψ as a function of CB content for fresh and Joule heating samples are recorded in Table I. From Table I, it is clear that the value of ψ increased with increasing CB and Joule heating. We believe that CB improved the packing density of the conductive site, and Joule heating enhanced the molecular texturing of the microstructure core of the epoxy matrix. This value indicates that the epoxy–CB composites showed stable NTCC characteristics, and they were more suitable for lower voltage applications.

The *I–V* curves in Figures 12 and 13 are described by the following empirical formula:[11]

$$I = \frac{V}{aV^3 + bc^{\phi}} \tag{18}$$

where aV^3 and bc^{ϕ} are resistances that depend on the applied potential and the dispersion of CB in the epoxy composites, respectively.

The calculated fitting parameters of eq. (18) for two batches of epoxy composites are recorded in Table I. The data recorded in Table I indicate that the CB and Joule heating enhanced the dispersion of CB within

TABLE I
Values of Non-Ohmic Coefficients and Calculated Fitting Parameters of Eq. (18) as a Function of CB Content for Fresh and Joule Heating Samples

Parameter	F4/6	F5/5	F6/4	F6.5/3.5	F7/3
a (amp)$^{-1}$					
Fresh	3.6×10^{-2}	4.2×10^{-2}	4.9×10^{-2}	5.6×10^{-2}	6.8×10^{-2}
Joule	3.9×10^{-2}	4.4×10^{-2}	5.6×10^{-2}	6.5×10^{-2}	7.6×10^{-2}
b (Ohm)					
Fresh	988,776	12850	800	176	43
Joule	510,948	9456	403	85	23
c					
Fresh	21.765	19.345	14.876	9.453	5.462
Joule	22.056	16.992	11.760	7.861	4.213
ψ					
Fresh	4.021	5.98	8.79	10.34	13.54
Joule	5.33	7.08	9.46	12.07	15.78

the epoxy matrix. In addition, the previous empirical formula was useful for the prediction of the variation of resistance with applied power for these composites from a technical point of view.

Temperature response to applied power

Figure 15 shows the working power versus ultimate surface temperature of all testes samples for the two batches. The surface temperature was strongly affected by CB content and the Joule heating treatment. Indeed, the temperature increased with increasing working power and depended on CB content. It markedly increased the temperature difference produced by Joule heating at the same applied electric power. This clue strongly supports the indication that CB improved the CLD and thermal stability of epoxy composites.

The surface temperature level of the Joule heating batch was higher than the fresh batch at the same applied power. This indicates that the Joule heating improved the thermodynamic equilibrium and thermal stability of the epoxy composites.

Checking the thermal stability under applied power

For comparison, Figure 16 presents the ultimate surface temperature and current versus time (T–t) during several thermal cycles under applied DC power, about 1 W on and off for fresh and Joule heating samples F6/4 and F6/4. It is clear that the surface temperature level of the Joule heating batch was higher than that of the fresh batch. The ultimate and initial temperatures of the Joule heating batch did not change under the on-and-off applied power cycle compared to those of the fresh batch. Also, the Joule heating modified the molecular architecture of the epoxy matrix. In conclusion, we think that the Joule heating caused an increase in the thermal capacity into the epoxy matrix and led to an increase in cycle life.

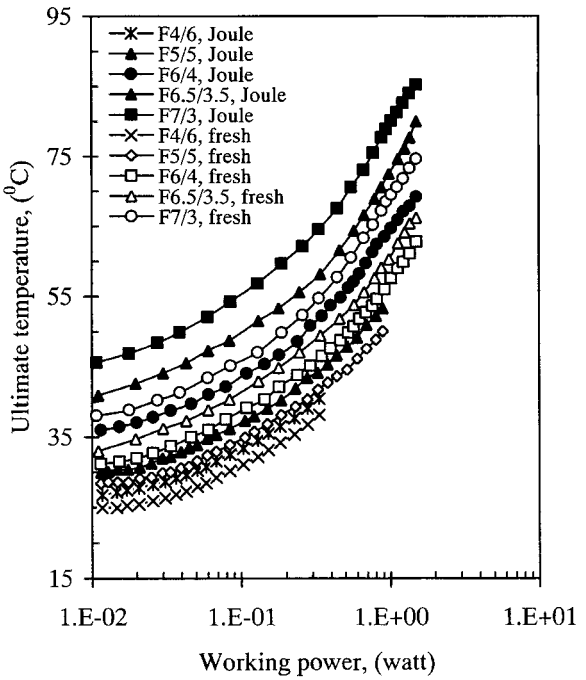

Figure 15 Working power–ultimate surface temperature dependence of fresh and Joule heating samples.

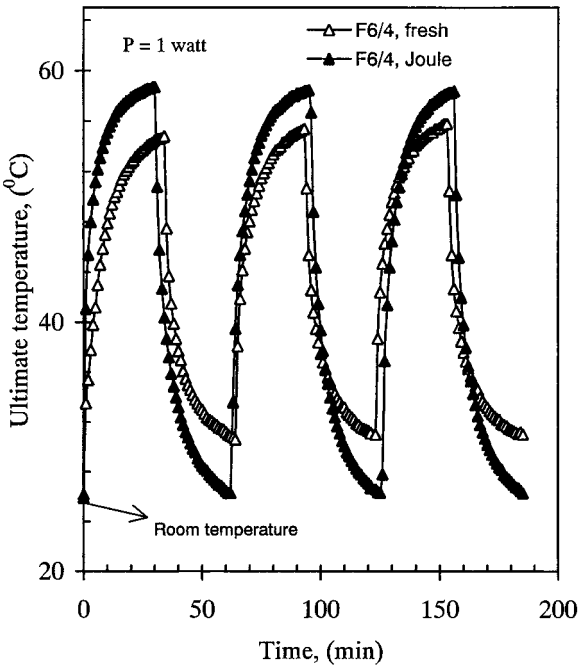

Figure 16 Ultimate surface temperature versus time during several thermal cycles under applied DC power of about 1 W on and off for fresh and Joule heating samples F6/4.

Specific heat (C_p) and amount of heat transfer (α) calculated with the energy balance concept

The T–I–t curve under applied power served to help us calculate some useful thermal parameters, such as C_p and the amount of total heat transferred including heat transfer by radiation and convection (α), based on the energy balance equation for the epoxy–CB composites for two batches. For calculating C_p and α, the temperature and current because of Joule heating of the epoxy samples were recorded as a function of time during the application of electric power on and off across the sample. During measurement, the initial applied power was kept constant until equilibrium temperature (i.e., room temperature) was reached.

The T–I–t curves for all of the tested samples under applied power of about 1 W are depicted in Figure 17. Figures 17 and 18 can be divided into three stages: (1) temperature growth (i.e., heating), (2) equilibrium

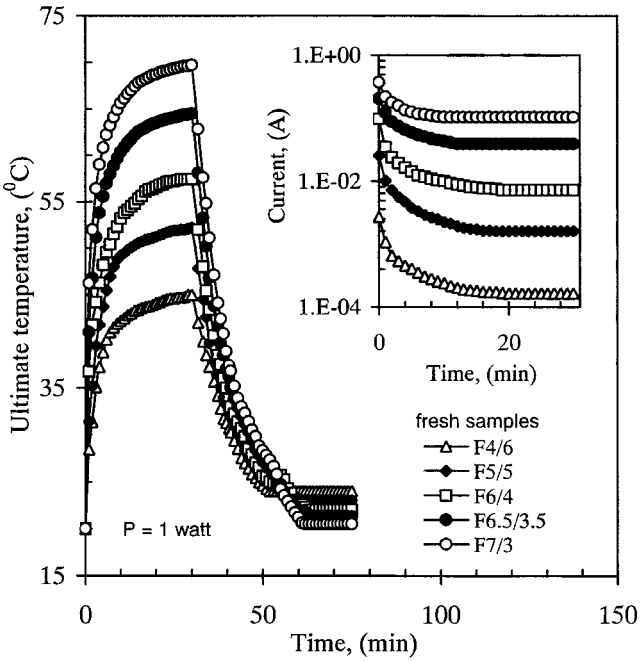

Figure 17 Temperature–time–current characteristics under applied power of 1 W on and off for fresh samples.

(i.e., saturation temperature), and (3) temperature decay (i.e., cooling when the power was off).

In stage 1, the electric field was applied to the sample; in this stage, the energy balance is given by[1,16]

$$I_m V_0 \int_{t_0}^{t_m} dt = mC_p(T_m - T_0) + A\alpha \int_{t_0}^{t_m} (1 - {}^{-e-(t/\tau_g)})\, dt \quad (19)$$

where I_m is the maximum current at time t_m; V_0 is the initial applied voltage; A is the area of the sample; m is the mass of the tested sample; T_m and T_0 are the maximum and initial temperatures, respectively; and τ_g is the characteristic growth time constant and is calculated by the following equation and is determined at $t = \tau_g$:

$$\left(\frac{T - T_0}{T_m - T_0}\right) = (1 - e^{-(t/\tau_g)}) \quad (20)$$

Variations of τ_g versus CB content for two batches are depicted in Figure 18.

Figure 17 shows the dependence of conduction current on time, which can be expressed by the following equation:[1,16]

$$\left(\frac{I_t - I_0}{I_m - I_0}\right) = \exp - \left(\frac{t}{t_i}\right) \quad (21)$$

where t_i is a characteristic current time constant, which depends on CB and the Joule heating effect.

Stage 2 was the case of the equilibrium state (i.e., heat gain by working power = heat loss by radiation and convection). In this stage, the conservation of energy equation can be written as follows:

$$(I_c V_0) = A\alpha(T_m - T_0) \quad (22)$$

where I_c is the steady state current, which depends on CB content and the Joule heating effect.

The variation of α as a function of CB content and Joule heating for the epoxy composites are illustrated in Figure 18. From eqs. (19–22), we get C_{pt} in the following equation:

$$C_{pI} = \left(\frac{1}{m(T_m - T_0)}\right)[V_0 t_c (T_m - T_0)] + \ln\left(\frac{t_c + t_i}{t_i}\right) + V_0 I_m t_c - A\alpha(T_m - T_0)(t_c - e^{-(t_c/\tau_g)}) \quad (23)$$

where τ_c is the time at which the current reaches I_c.

Finally, in stage 3, during which the working power was switched off, and the sample was left to cool down by radiation and convection according to Newton's law of cooling. In this stage, the temperature varied with time according the empirical formula

$$\left(\frac{T_t - T_0}{T_m - T_0}\right) = e^{-(t/\tau_d)} \quad (24)$$

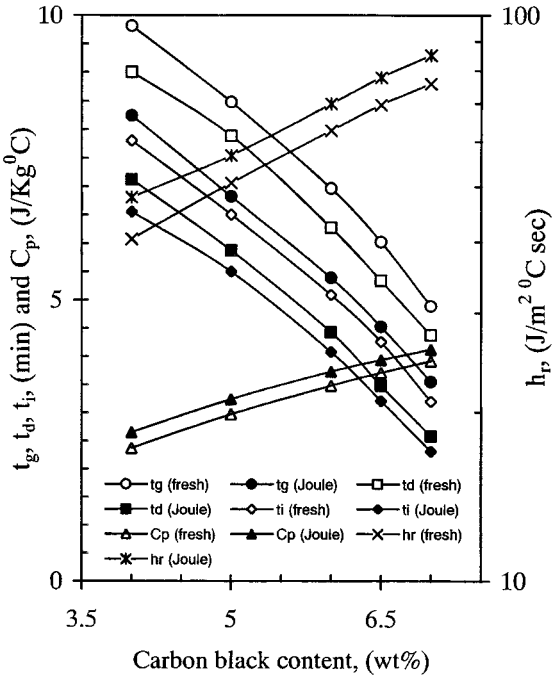

Figure 18 Calculated values of C_p, amount of heat transfer, characteristic time growth, decay, and current constant versus CB content for two batches of epoxy composites.

where τ_d is a characteristic decay time constant, which depends on CB content and the Joule heating effect.

The conservation law of energy in stage 3 yielded the following equation:

$$mC_{pIII}(T_m - T_0) = A\alpha(T_m - T_0) \int_{\tau_d}^{t_0} e^{-(t/\tau_d)}\, dt \tag{25}$$

where t_0 is the required time for the temperature of the sample to attain T_0 and I_c; therefore

$$C_{pIII} = \frac{1}{m}(A\alpha\tau_d)(1 - e^{-(t_0/\tau_d)}) \tag{26}$$

The calculated values of C_p against CB content for two batches are depicted in Figure 18. From these results, one can understand that with the calculated values of α per unit sample area per second one can control the optimum working conditions to warm a given volume at a given initial boundary condition. The values of C_p were in good agreement with the previous results obtained for polymer composites.[1,16] τ_g and τ_d decreased with increasing CB content and Joule heating. This means that the Joule heating treatments improved the dispersion and alignment of CB particles into the epoxy matrix.

CONCLUSIONS

1. In this work, for the first time the effects of Joule heating on network structure, σ, and thermal stability of epoxy–CB composites were measured experimentally. Joule heating and CB content enhanced the network structure density and molecular architecture of epoxy–CB composites.
2. σ of epoxy–CB composites at room temperature could be adjusted by the monitoring of the CB content. The Joule heating effect increased σ, certainly due to an increase in conductive paths of the CB domains in the epoxy matrix.
3. σ increased with increasing temperature and strongly depended on the CB content and Joule heating. The hopping process governed the electrical conduction mechanism of this composite. The charge carrier's transport was the hole.
4. The thermal stability of the epoxy was affected by the loading of the CB, which was relatively more stable with increasing CB content in the composite.
5. C_p and the amount of heat transfer by radiation and convection depended on CB content and Joule heating.
6. Conductivity cycles and temperature–time under applied power indicated that the Joule heating effect is a very effective and prospective way for improving the thermal reliability of epoxy–CB composites for consumer use as heating elements.
7. This findings might accelerate the use of the Joule heating as a new and rapid way for enhancing the electrical and thermal stability of conductive polymer composites.

The authors would like to thank all staff members in the Faculty of Engineering and Faculty of Science, Niigata University, Japan for their kind encouragements. F. E.-T. thanks Prof. Dr. M. Hisada, Department of Civil Engineering, Niigata University, Japan for providing the necessary equipments to carry out SEM and thermal analysis.

References

1. El-Tantawy, F. Eur Polym J 2001, 37, 565.
2. Kagathara, V. M.; Sanariya, M. R.; Parsania, P. H. Eur Polym J 2000, 36, 2371.
3. Lundberg, B.; Sundqvist, B. J Appl Phys 1986, 60, 1074.
4. El-Tantawy, F.; Bakry, A.; El-Gohary, A. R. Polym Int 2000, 49, 432.
5. Bera, S. K.; Chaudhuri, S.; Pal, A. K. J Phys D: Appl Phys 2000, 33, 2320.
6. Petrovsky, V. Y.; Rak, Z. S. J Eur Ceram Soc 2000, 21, 237.
7. Calberg, C.; Blacher, S.; Gubbles, F. J Phys D: Appl Phys 1999, 32, 1517.
8. Chalterjee, S.; Sengupta, K.; Naiti, H. S. Sens Actuators B 2000, 60, 155.
9. Brzozowski, E.; Castro, M. S. Ceram Int 2000, 26, 265.
10. Kokabi, H. R.; Rapeaux, M.; Aymami, J. A.; Desgardin, G. Mater Sci Eng B 1996, 38, 80.
11. Fujikura, Y.; Kawarai, M.; Ozaki, F. Polymer J 1989, 21, 8609.
12. Prokes, J.; Krivka, I.; Tobolkova, E.; Stejskal, J. Polym Degrad Stab 2000, 68, 261.
13. Dhami, A. K.; Chattopadhyay, M. K.; Dey, T. K. J Supercond 2000, 13, 3.
14. Kutty, T. R. N.; Philip, S. Mater Sci Eng B 1995, 33, 58.
15. Ishikawa, H.; Satoh, M. J Phys D: Appl Phys 1992, 25, 897.
16. Hassan, H. H.; Abdel-Bary, E. M.; El-Mansy, M. K.; Shash, N. M. Appl Phys Commun 1989–1990, 9, 267.